Repriming and activation alter the frequency of stereotyped discrete Ca²⁺ release events in frog skeletal muscle

Alain Lacampagne, W. Jonathan Lederer, Martin F. Schneider *
and Michael G. Klein

*Department of Biochemistry and Molecular Biology and Department of Physiology,
University of Maryland School of Medicine, 108 North Greene Street, Baltimore,
MD 21201, USA*

1. Brief localized elevations in myoplasmic $[Ca^{2+}]$ (Ca^{2+} sparks) in individual sarcomeres of voltage-clamped frog skeletal muscle fibres were examined by laser scanning confocal microscopy.

2. Fibres held at 0 mV were briefly repolarized to −90 mV (repriming pulse) to restore only a small fraction of sarcoplasmic reticulum (SR) calcium release. Subsequent depolarization to 0 mV (test pulse) caused the appearance of small numbers of Ca^{2+} sparks at different sarcomeres from pulse to pulse. Increasing the repriming time resulted in an increase in the frequency of occurrence of the Ca^{2+} sparks.

3. The amplitude and spatio-temporal extent of the Ca^{2+} sparks were independent of the repriming time and test pulse voltage. Ca^{2+} sparks recorded during small depolarizations of fibres held at −90 mV had a similar amplitude and spatio-temporal extent as those recorded after brief repriming of the same fibre held at 0 mV.

4. We conclude that stereotyped Ca^{2+} sparks underlie calcium release at all voltages and all extents of repriming. The amplitude of Ca^{2+} release is thus graded by the frequency but not by the amplitude or spatio-temporal extent of the individual SR Ca^{2+} release events.

Depolarization of a skeletal muscle fibre causes calcium release from the sarcoplasmic reticulum (SR), resulting in fibre contraction. This depolarization activates voltage sensor molecules in the transverse tubule (TT) membrane that control the opening of Ca^{2+} release channels in the closely apposed SR junctional face membrane (Schneider & Chandler, 1973; Rios & Pizzaro, 1991; Schneider, 1994). The resulting Ca^{2+} efflux from the SR has recently been detected as brief localized elevations of cytosolic $[Ca^{2+}]$ (Ca^{2+} 'sparks') that increase steeply in frequency with increasing depolarization in voltage-clamped frog skeletal muscle fibres (Tsugorka, Rios & Blatter, 1995; Klein, Cheng, Santana, Jiang, Lederer & Schneider, 1996). Such Ca^{2+} sparks, activated by depolarization, are presumably initiated by conformational changes in the TT voltage sensors and are attributed to the Ca^{2+} efflux through single SR Ca^{2+} release channels or a few channels acting as a single functional unit. The local elevation of $[Ca^{2+}]$ during a Ca^{2+} spark corresponds to a small fraction of the $[Ca^{2+}]$ that is achieved during larger depolarizations, which cause more complete activation of

release (Schneider & Klein, 1996). Ca^{2+} sparks become indistinguishable in the macroscopic $[Ca^{2+}]$ transient for even modest depolarizations, reflecting the growing overlap of Ca^{2+} sparks with greater activation (Tsugorka *et al.* 1995; Klein *et al.* 1996).

Here we investigate Ca^{2+} sparks over the full voltage range of activation of Ca^{2+} release. By fully inactivating the TT voltage sensors and then repriming a small fraction (Hodgkin & Horowicz, 1960; Adrian, Chandler & Rakowski, 1976; Chandler, Rakowski & Schneider, 1976) we establish conditions that permit large depolarizations of fibres without producing a massive calcium release that would obscure individual SR Ca^{2+} release events. Under these conditions Ca^{2+} sparks can be resolved over the full range of depolarizations. Our results indicate that similar discrete SR Ca^{2+} release events underlie Ca^{2+} release at all depolarizations and that the level of release is graded by the frequency but not the amplitude or spatio-temporal extent of the discrete events.

METHODS

The methods for muscle fibre preparation, mounting and voltage clamping were similar to those described previously (Kovacs, Rios & Schneider, 1983; Klein *et al.* 1996; Schneider & Klein, 1996). Briefly, frogs (*Rana pipiens*) were killed by decapitation and spinal cord destruction. Single fibre segments from the ileofibularis muscle were isolated in a relaxing solution containing (mM): 120 potassium glutamate, 2 $MgCl_2$, 0·01 EGTA, 5 sodium tris-maleate; pH 7·0. They were mounted in a double Vaseline gap chamber (Schneider & Klein, 1996) at a sarcomere spacing of 3·2–3·6 μm. The fibre regions within the end pools were permeabilized by a brief exposure to 0·01 % w/v saponin in relaxing solution (Irving, Maylie, Sizto & Chandler, 1987). The end pools were changed to 'internal' solution containing (mM): 80 caesium glutamate, 5·5 $MgCl_2$, 5 Na_2ATP, 4·5 sodium tris-maleate, 13·2 caesium tris-maleate, 0·1 EGTA, 0·008 $CaCl_2$, 20 creatine phosphate (disodium salt), 5 glucose and 100 μM fluo-3 (pentapotassium salt); pH 7·0; and the central pool was changed to 'external' solution containing (mM): 125 TEA-methanesulphonate, 5 Cs-Hepes, 2 $CaCl_2$ and 3×10^{-4} TTX; pH 7·0. Fibres were voltage clamped at a holding potential of 0 mV for at least 30 s before each repriming pulse. Experiments were carried out at room temperature (*ca* 23 °C). All chemicals were from Sigma, except for glutamic acid (Aldrich) and fluo-3 (Molecular Probes).

Fibres were mounted just above the coverslip floor of the chamber, which was clamped to the stage of an inverted microscope (Olympus IX-70 with Olympus ×60, 1·4 NA oil objective). Fibre fluorescence was monitored using a Bio-Rad MRC 600 laser scanning confocal system operating in line-scan mode (*x vs. t*). The laser spot scanned a line along the fibre axis once every 2 ms. The confocal pinhole was set to *ca* 25 % of maximum, giving an optical resolution of *ca* 0·4 μm in the *x* and *y* dimensions, and 0·8 μm in the *z* (vertical) dimension (full-width at half-maximum (FWHM); determined by imaging sub-resolution fluorescent beads).

Fluorescence line-scan images were converted to images of changes in fluorescence (ΔF) by subtracting the average fluorescence pattern measured along the scan line during the repriming intervals (before the test pulse) of four repriming episodes within a given run (see Fig. 1). Each ΔF image in the run was then converted to a line-scan image of $\Delta F/F$ by dividing by the mean resting fluorescence (F) averaged over all pixels along the scan line during the repriming intervals. Individual Ca^{2+} sparks were identified by interactively superimposing a rectangle (dimensions: 3·3 μm in *x*, 20 ms in *t*) on the pseudocolour video display of a $\Delta F/F$ line-scan image, with simultaneous display of the average time course and spatial profile within the rectangle. An event was identified as a temporally isolated elevation of fluorescence of at least 0·5 units of $\Delta F/F$, with a spatial extent (FWHM) greater than 1 μm, and a time course (FWHM) greater than 6 ms but less than 20 ms for temporal isolation. Using these criteria, the identification of Ca^{2+} release events in a series of images by several individuals was quite similar (Klein *et al.* 1996). Note that the video pseudocolour representation of the $\Delta F/F$ images was slightly different from the colour figures presented in this paper due to variations in colour reproduction. Averaged Ca^{2+} sparks for a given repriming duration and test pulse voltage were calculated by averaging line-scan images of individual, temporally isolated sparks recorded during the test pulse of a given pulse sequence. Individual sparks were shifted in time so as to synchronize all events at the time to half-peak, spatially superimposed, averaged and displayed as surface plots of $\Delta F/F$.

RESULTS

Figure 1*A* (top) illustrates the voltage protocol of an episode used to reprime and then activate a small number of voltage sensors. Fibres were held at 0 mV to fully inactivate the TT voltage sensors (Chandler *et al.* 1976). A small fraction of the voltage sensors was restored from inactivation using a relatively brief (190 ms in Fig. 1) repriming pulse to −90 mV (Adrian *et al.* 1976), which was followed immediately by a test pulse depolarization (500 ms to 0 mV in Fig. 1) to produce near full activation of any reprimed voltage sensors (Chandler *et al.* 1976). A 100 ms step back to −90 mV next deactivated the voltage sensors and a final step back to the 0 mV holding potential reactivated and then inactivated the reprimed voltage sensors before starting the next repriming episode at least 30 s later.

The image in Fig. 1*A* is the line-scan image of fibre fluorescence, with time on the horizontal axis (synchronized with the pulse protocol above), distance along the scan line on the vertical axis and fluorescence represented in pseudocolour. The line-scan image shows five obvious instances in which the fluorescence in a highly localized region along the scan line became briefly elevated, corresponding to spatially discrete local elevations of $[Ca^{2+}]$ or Ca^{2+} sparks. These five Ca^{2+} sparks occurred along two horizontal bands (see arrowheads). The fluorescence intensity along the scan line image in the resting fibre during the repriming period in Fig. 1*A* exhibited a periodic spatial variation (Fig. 1*A*, right), which continues throughout the line scan image in Fig. 1*A* as a set of parallel, approximately equally spaced, darker and lighter bands. The periodicity of this pattern corresponds to the striation spacing of the fibre, with the TT location being at the centre of the dark band (Klein *et al.* 1996). The upper three sparks are centred exactly on the dark band of the resting fluorescence pattern of the fibre (Klein *et al.* 1996), as expected for the junctional SR origin of the release channel or channels giving rise to the spark. The bottom two sparks are in a region where the resting pattern was less apparent and thus cannot be assigned to either band.

The fluorescence image in Fig. 1*A* was used to calculate the corresponding $\Delta F/F$ line-scan image in Fig. 1*B*. Such $\Delta F/F$ images were used for spark identification and characterization. The $\Delta F/F$ image in Fig. 1*B* exhibits the same five sparks as identified in the raw fluorescence image in Fig. 1*A*, as well as one other event fulfilling the event selection criteria (see Methods). The time courses of $\Delta F/F$, monitored at the two locations of repeated events in the Fig. 1*B* image, are shown in the top and bottom single sarcomere $\Delta F/F$ records in Fig. 1*B* (right). The three events in the top record (two during the first depolarization and one during the second) and the two events in the bottom record (both during the first depolarization) are obvious in the single sarcomere records. These events exhibited very similar spatial extents along the sarcomere (vertical) and

very similar temporal durations (horizontal) in the Fig. 1*B* $\Delta F/F$ line-scan image. The middle two single sarcomere records in Fig. 1*B* showed no activity and there was no indication of sparks at the corresponding location in the Fig. 1*B* image (middle two arrowheads). The peak amplitude of the discrete events in the single sarcomere records is many times greater than the mean elevation of $\Delta F/F$ during the depolarization, which was negligible (not shown). Most sarcomeres in the Fig. 1*B* image exhibited no detectable spark activity after this relatively short repriming time. However, all sarcomeres exhibited release when the repriming time was increased in this fibre (not shown).

The $\Delta F/F$ line-scan images (Fig. 1*C* and *D*) for two successive applications of the same pulse protocol as in Fig. 1*A* and *B* again exhibited a few Ca²⁺ sparks. The sparks occurred in different sarcomeres and at different times during the depolarization of each repriming episode (Fig. 1*B–D*). This is as expected for independent stochastic repriming of a small random sample of voltage sensors during each repriming episode from a large population of inactivated voltage sensors distributed among all sarcomeres. The $\Delta F/F$ records for the same four single sarcomeres as in Fig. 1*B* showed that the two sarcomeres inactive in Fig. 1*B* had events in either Fig. 1*C* or *D* (right) and that only the
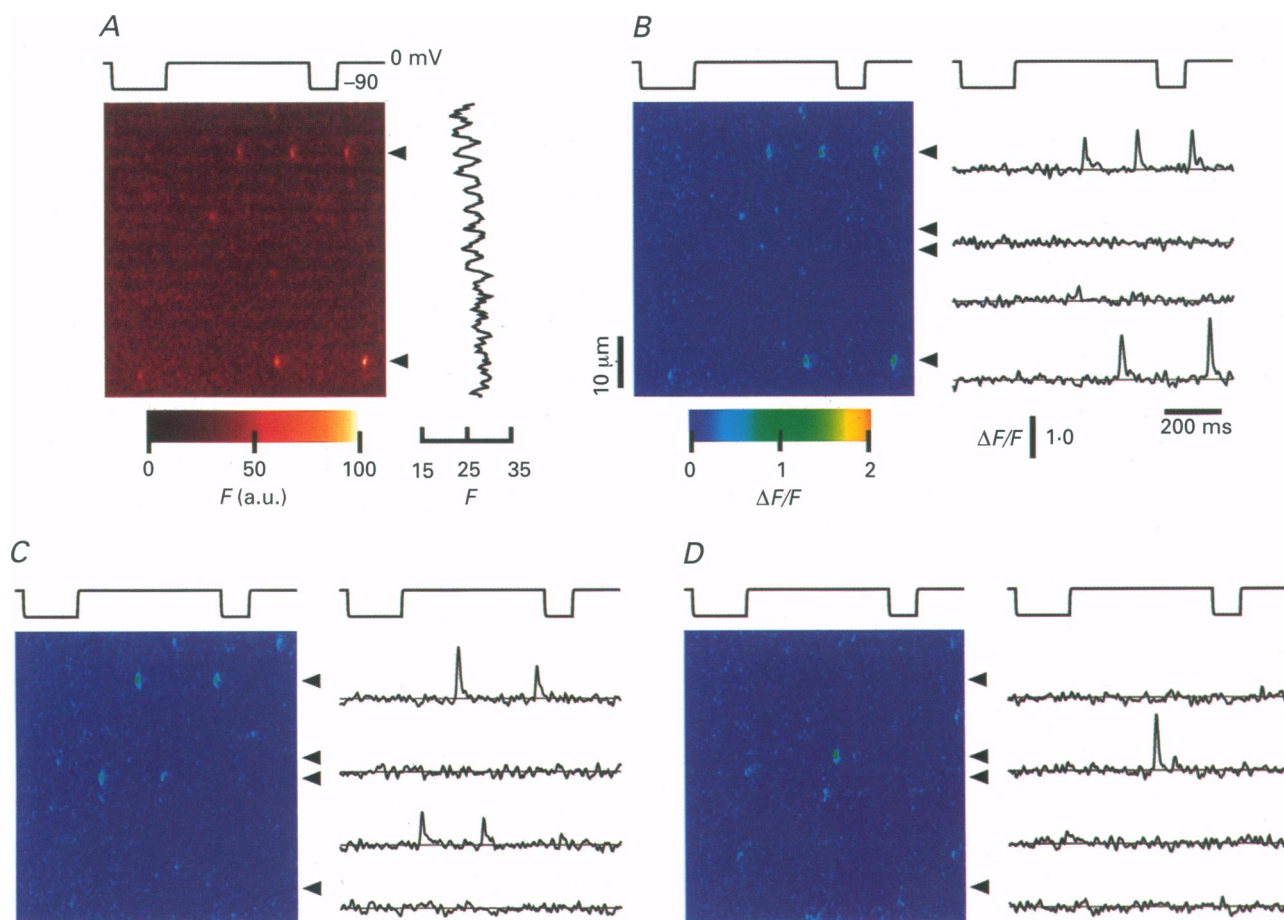
Figure 1. Ca²⁺ release events activated after brief repriming of a fully depolarized fibre

A, confocal line-scan image (left) of total fibre fluorescence (pseudocolour; arbitrary units, a.u.) along a line (vertical) parallel to the fibre axis during the voltage-clamp pulse protocol above the image (same time scale as the horizontal dimension in the image). Several discrete release events are evident during the first or second depolarizations. Five events are localized within two individual sarcomeres (arrowheads), identified from the fluorescence pattern along the scan line (right) during the repriming interval, averaged from four applications of the pulse protocol. *B*, left, the $\Delta F/F$ calculated from the fluorescence image in *A*; right, records of the time course of $\Delta F/F$ within four selected individual sarcomeres (arrowheads). *C* and *D*, line-scan images of $\Delta F/F$ (left) from two subsequent applications of the same repriming protocol as in *A* and *B*; and records (right) of $\Delta F/F$ from these images for the same four sarcomeres as selected and identified in *B* (arrowheads). Same format as *B*. Note the activation of Ca²⁺ release events in different sarcomeres, and at different times in each pulse sequence.
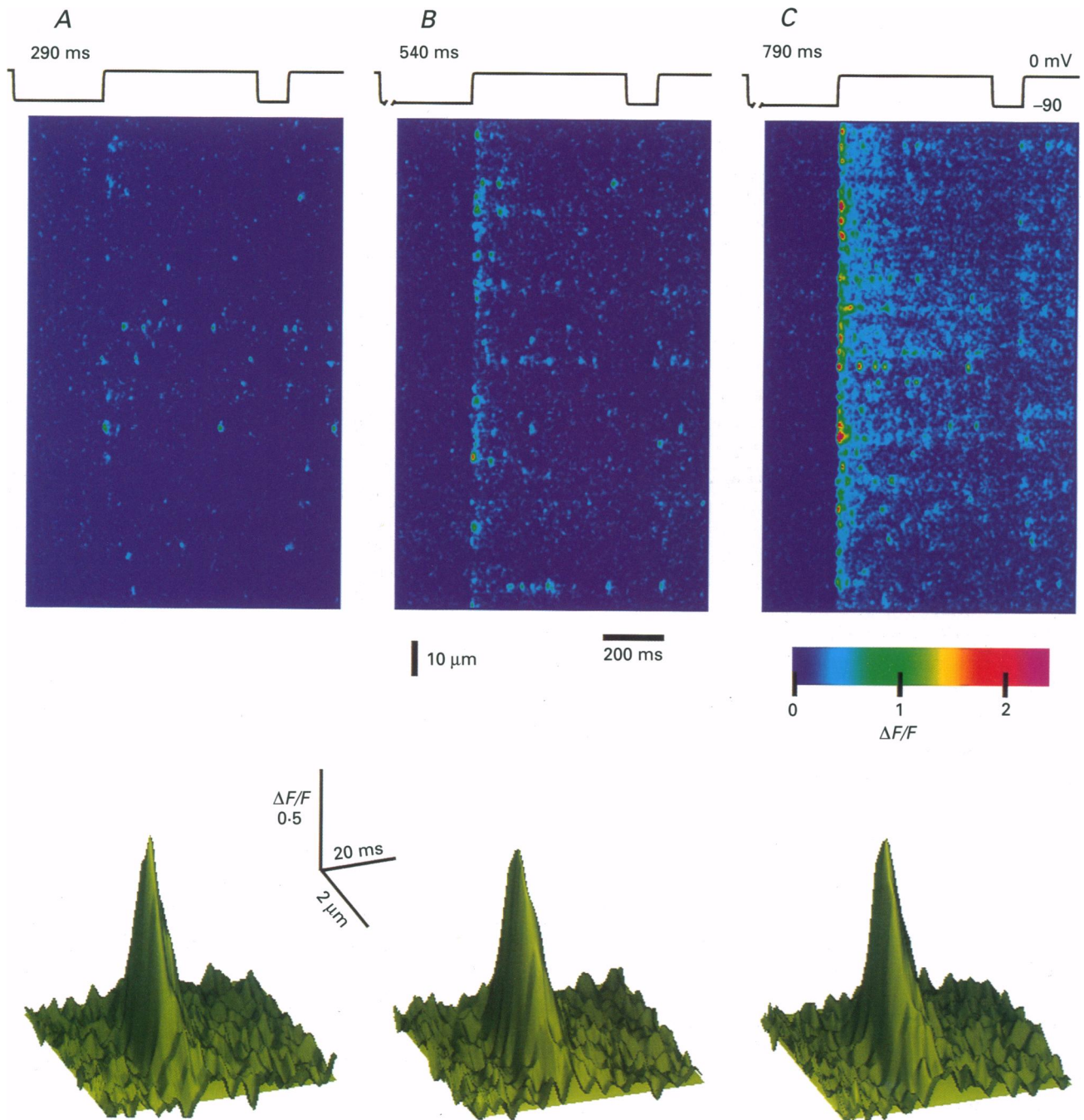
Figure 2. The effect of repriming duration on the activation of Ca^{2+} release events

Upper panels, repriming intervals of 290 ms (*A*), 540 ms (*B*) and 790 ms (*C*) result in the activation of greater numbers of Ca^{2+} release events, as the repriming time is increased. The pulse protocol is shown above each line-scan image. The lower panels show the average of Ca^{2+} sparks activated after each of the different repriming intervals (*A–C*), calculated as described in Methods. To minimize the inclusion of coincident events in the average, for the 540 and 790 ms repriming intervals only Ca^{2+} release events occurring later than 200 ms after the start of the test pulse were included in the analysis. The averaged Ca^{2+} sparks are very similar in amplitude and spatio-temporal extent. Number of events averaged: 52 (*A*), 80 (*B*), 86 (*C*).

sarcomere marked by the uppermost arrowhead exhibited events in more than one repriming episode. The events in the single sarcomere records in Fig. 1*B–D* exhibited similar spatio-temporal extents in the corresponding line-scan images (see arrowheads). Several other sparks were detected in Fig. 1*B–D* and had similar time courses in single sarcomere records (not shown) to those in the single sarcomere records in Fig. 1. These observations indicate that repriming of small numbers of voltage sensors allows detection and characterization of discrete Ca²⁺ sparks produced by voltage sensor activation during large depolarizations.

Figure 2 examines the effects of repriming time on release events during a test pulse to 0 mV in another fibre. Increasing the repriming time from 290 ms (Fig. 2*A*) to 540 ms (Fig. 2*B*) and 790 ms (Fig. 2*C*) resulted in a progressive increase in the frequency of occurrence of Ca²⁺ sparks in the Δ*F*/*F* line-scan images (top) and in the average fluorescence change during the test pulse (not shown). For the 540 and 790 ms repriming times (Fig. 2*B* and *C*), the event frequency became sufficiently large early in the test pulse that individual events could not be distinguished in the large early increase in fluorescence. However, for both these repriming durations, individual events could be identified later in the pulse as the event frequency declined during the test pulse, presumably due to release inactivation (Schneider & Simon, 1988). Despite the large increase in frequency with increasing repriming, the amplitude and spatio-temporal extent of the averaged events (Fig. 2, bottom) were remarkably similar for each of these three different extents of repriming.

Figure 3 explores the effect of test pulse voltage on the discrete release events. The Δ*F*/*F* line-scan images (top) in Fig. 3*A* and *B* show events occurring during a test pulse to 0 mV after 790 ms repriming at −90 mV (Fig. 3*A*) and during a test pulse to −40 mV after 2 s repriming at −90 mV (Fig. 3*B*). The amplitude and spatio-temporal extent of the averaged Ca²⁺ spark were very similar for the test pulses to −40 and 0 mV (Fig. 3*A* and *B*, middle). The event frequency was much greater during the test pulse to 0 mV after 790 ms repriming at −90 mV (Fig. 3*A*) than during the test pulse to −40 mV after the longer 2 s repriming at −90 mV (Fig. 3*B*). However, the much larger fluorescence increase during the final step to 0 mV in Fig. 3*B* than during the test pulse to the same 0 mV potential demonstrates that the extent of repriming was considerably greater in Fig. 3*B* than in Fig. 3*A*. Note also that both Fig. 3*A* and *B* were obtained from the same fibre as in Fig. 2, but later in the experiment. The lower event frequency and average fluorescence observed for the same repriming and test pulse combination in Fig. 3*A* compared with Fig. 2*B* indicates some fibre run-down. Even so, the averaged event (Figs 3*A*, middle and 2*B*, bottom) was still remarkably constant for these two figures.

Figure 3*C* and *D* illustrates the effects of more extreme reciprocal increased repriming and decreased test pulse depolarization in another fibre. Here a relatively low frequency of events was observed during a test pulse to 0 mV after 190 ms repriming at −90 mV and during a test pulse to −65 mV with the fibre held at −90 mV, which in effect corresponds to an infinite repriming time at −90 mV. The averaged events in Fig. 3*C* and *D* (middle) were again very similar for each of these very different conditions of repriming time and test voltage. Thus the averaged discrete Ca²⁺ release events appear to be closely similar for different extents of repriming and different test depolarizations in a given fibre.

The entire test pulse interval of each Δ*F*/*F* line-scan image in Fig. 3 is shown at double spatio-temporal magnification in the bottom row of Fig. 3. Each individual event in the magnified image that was used in calculating the averaged event is shown enclosed in the rectangular spatio-temporal box used for event selection (see Methods).

Figure 4 examines the mean values of peak amplitude (Fig. 4*A*), duration at half-peak ('half-duration', Fig. 4*B*) and spatial extent along the sarcomere at half-peak ('half-width', Fig. 4*C*) of Ca²⁺ sparks recorded in four different fibres, each represented by a different symbol, over a relatively wide range of test pulse voltages. The values of peak Δ*F*/*F* for each fibre were independent of the test voltage, but varied somewhat between fibres, perhaps due to differences in resting [Ca²⁺] causing differences in dye responsiveness or perhaps reflecting actual differences in amount of Ca²⁺ released per spark in different fibres. The values of the temporal half-duration and spatial half-width were essentially constant over the full range of test pulse voltages at which Ca²⁺ sparks were recorded. Thus the amplitude and spatio-temporal extent of the Ca²⁺ sparks were independent of the voltage at which they were activated. The spatial half-width was also remarkably similar between fibres (Fig. 4*C*). The mean value of peak amplitude reported here is slightly larger and the mean half-time and mean half-width are slightly smaller than we reported previously (Klein *et al.* 1996). Improved optics and the low background fluorescence in the repriming protocol results in higher signal-to-noise line-scan images of Ca²⁺ sparks and presumably now allows more accurate estimation of these parameters than previously.

DISCUSSION

This paper presents the first recordings of Ca²⁺ sparks at large depolarizations in skeletal muscle. This was achieved by first inactivating all TT voltage sensors and then repriming only a small number prior to each test depolarization. A similar repriming protocol was used by Adrian *et al.* (1976) to study the restoration of mechanical activity after prolonged depolarization of skeletal muscle fibres. In the present experiments low repriming was
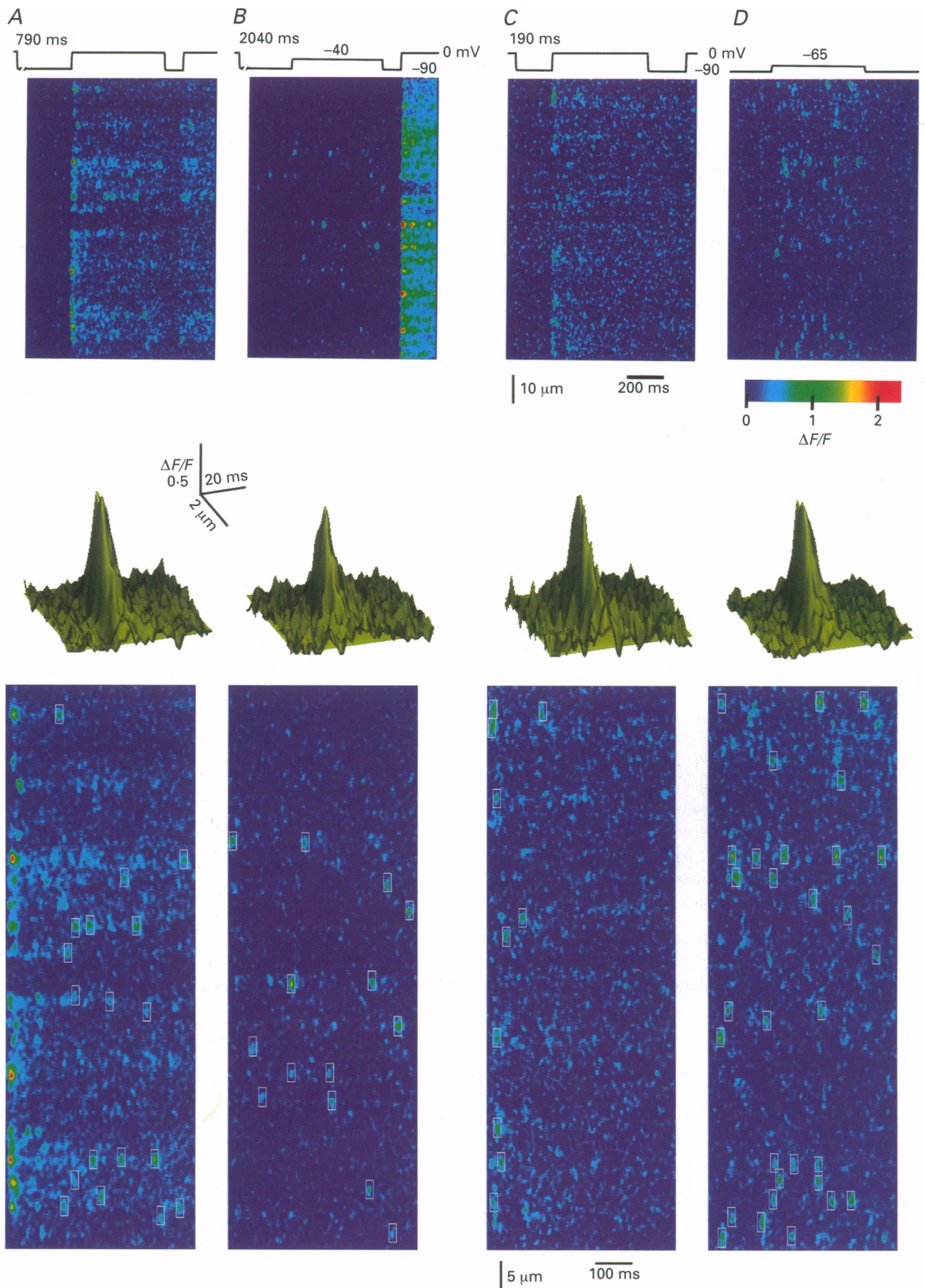
Figure 3. For legend see facing page.

Figure 4. Mean values of Ca²⁺ spark peak amplitude (*A*), duration at half-peak (*B*) and longitudinal spread along sarcomere at half-peak (*C*) are independent of the test voltage

Each symbol gives results from a different fibre. The filled symbols give values for the fibre held at −90 mV and the open symbols are for repriming runs in the same fibre held at 0 mV. Error bars denote 1 s.e.m. If not shown, the s.e.m. was smaller than the symbol. Each value is mean of values from 10 to 139 individual Ca²⁺ sparks at the indicated membrane potential in one fibre. Slopes of regression lines fitted to data in each panel were not significantly different from 0 (not shown).
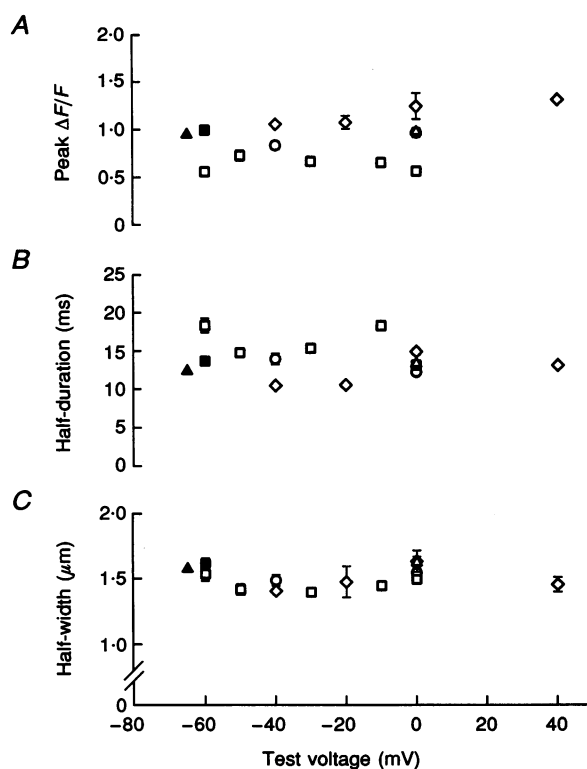
utilized, so that the large [Ca²⁺] transient that would otherwise occur during large depolarizations of a fully activated fibre was prevented from obscuring individual sparks. Conditions of very low repriming are also ideal for resolving individual Ca²⁺ sparks since the likelihood of superimposed events is low. It is thus possible to show that the amplitude and spatio-temporal extent of the averaged Ca²⁺ sparks are independent of both the test depolarization and the extent of repriming, and were similar in partially and fully reprimed fibres. Consequently, the large increase in overall Ca²⁺ release observed with increasing depolarization in fully polarized fibres appears to result from increased frequency of occurrence of stereotyped Ca²⁺ sparks rather than a voltage-dependent change in the individual events.

In a previous paper, a class of unitary amplitude events was distinguished from classes of double and triple amplitude events (Klein *et al.* 1996). A similar classification of the events

was not possible here, because estimates of the spontaneous event amplitude, which defined the unitary event amplitude in the previous study, were not obtained. However, if unitary and multiple amplitude events were present in the groups of Ca²⁺ sparks recorded here after various extents of repriming and various test depolarizations, the finding of similar averaged Ca²⁺ sparks for these various conditions would indicate that the proportion of unitary and multiple amplitude events must have been similar for the various conditions studied.

All processed line-scan images and all single sarcomere records presented here are expressed in units of Δ*F*/*F*, without converting to [Ca²⁺]. This avoids uncertainties in indicator calibration and kinetics and in resting [Ca²⁺], and provides a convenient means for comparing results from different fibres having different indicator concentrations. However, the Δ*F*/*F* signals are sufficient to establish that the

---

Figure 3. Discrete Ca²⁺ release events resolved at various voltages by reciprocal variation of repriming time and test depolarization

A and *B*, results for 500 ms test pulses to 0 mV after 790 ms repriming (*A*) or to −40 mV after 2040 ms repriming (*B*) in the same fibre as in Fig. 2, but 13 min later in the experiment. *C* and *D*, results for 500 ms test pulses to 0 mV after 190 ms repriming (*C*) or to −65 mV from a holding potential of −90 mV (*D*) in a different fibre than in *A* and *B*. Top, line-scan images of Δ*F*/*F*. Middle, average of Ca²⁺ sparks during the respective test pulses (*B*, *C*, *D*) or starting 200 ms after the start of the test pulse (*A*). Averaged events are means of 71 (*A*), 40 (*B*), 38 (*C*) and 85 (*D*) individual sparks, including all events outlined by boxes in the 2-times-magnified bottom images as well as events from three or more other images for the same protocol in the same fibre. Bottom, test pulse segment of each line-scan image at top, magnified about two times in both spatial and temporal dimension, and with sparks included in the average event enclosed in selection rectangles.

Ca^{2+} sparks were independent of voltage and repriming in a given fibre, indicating that the underlying Ca^{2+} release and $[Ca^{2+}]$ distribution were also the same. This is consistent with the channel opening events giving rise to the Ca^{2+} sparks being independent of these variables. As an approximate conversion from $\Delta F/F$ to $\Delta[Ca^{2+}]$, if the assumptions given in Klein et al. (1996) regarding the resting myoplasmic $[Ca^{2+}]$ and the binding of Ca^{2+} and fluo-3 apply, then one unit of $\Delta F/F$ corresponds to a change of $[Ca^{2+}]$ of 120 nM.

The present observations raise a provocative question. During a large depolarization, any reprimed TT voltage sensors should enter and remain in their activated conformation until the slow inactivation of charge movement (Chandler et al. 1976). However, our recordings of Ca^{2+} sparks show that SR Ca^{2+} release channels open only for a few milliseconds, as indicated by the duration of the rising phase of the Ca^{2+} sparks. What, then, is the mechanism for channel closure during maintained voltage sensor activation? At least four possibilities can be imagined for the channel closing mechanism: (i) the voltage sensor undergoes a voltage-insensitive conformational change that allows SR channel closure but does not alter charge movement; (ii) a conformational change in the SR channel as a consequence of channel activation; (iii) the activated voltage sensor permits the SR channel to open and close stochastically, dependent on the influence of all ambient modulators (Fleischer & Inui, 1989; Meissner, 1994); (iv) $[Ca^{2+}]$-dependent inactivation of the SR channel after it opens (Schneider & Simon, 1988). Although we cannot distinguish between these possibilities based on the present results, each of these possibilities implicates interesting local control mechanisms at the level of the voltage sensor–release channel complex. The present results do demonstrate that SR Ca^{2+} release channel gating can be studied in situ in skeletal muscle fibres from the pattern of occurrence of Ca^{2+} sparks.

ADRIAN, R. H., CHANDLER, W. K. & RAKOWSKI, R. F. (1976). Charge movement and mechanical repriming in striated muscle. *Journal of Physiology* **254**, 361–688.

CHANDLER, W. K., RAKOWSKI, R. F. & SCHNEIDER, M. F. (1976). Effects of glycerol treatment and maintained depolarization on charge movement in muscle. *Journal of Physiology* **254**, 285–316.

FLEISHER, S. & INUI, M. (1989). Biochemistry and biophysics of excitation–contraction coupling. *Annual Review of Biophysics and Biophysical Chemistry* **18**, 333–364.

HODGKIN, A. L. & HOROWICZ, P. (1960). Potassium contractures in single muscle fibres. *Journal of Physiology* **153**, 386–403.

IRVING, M., MAYLIE, J., SIZTO, N. L. & CHANDLER, W. K. (1987). Intrinsic optical and passive electrical properties of cut frog twitch fibers. *Journal of General Physiology* **89**, 1–40.

KLEIN, M. G., CHENG, H., SANTANA, L. F., JIANG, Y.-H., LEDERER, W. J. & SCHNEIDER, M. F. (1996). Two mechanisms of quantized calcium release in skeletal muscle. *Nature* **379**, 455–458.

KOVACS, L., RIOS, E. & SCHNEIDER, M. F. (1983). Measurement and modification of free calcium transients in frog skeletal muscle fibres by a metallochromic indicator dye. *Journal of Physiology* **343**, 161–196.

MEISSNER, G. (1994). Ryanodine receptor/Ca^{2+} release channels and their regulation by endogenous effectors. *Annual Review of Physiology* **56**, 485–508.

RIOS, E. & PIZARRO, G. (1991). Voltage sensor of excitation–contraction coupling in skeletal muscle. *Physiological Reviews* **71**, 849–908.

SCHNEIDER, M. F. (1994). Control of calcium release in functioning muscle fibers. *Annual Review of Physiology* **56**, 463–484.

SCHNEIDER, M. F. & CHANDLER, W. K. (1973). Voltage dependent charge movement in skeletal muscle. *Nature* **242**, 244–246.

SCHNEIDER, M. F. & KLEIN, M. G. (1996). Sarcomeric calcium sparks activated by fiber depolarization and by cytosolic Ca^{2+} in skeletal muscle. *Cell Calcium* **20**, 123–128.

SCHNEIDER, M. F. & SIMON, B. J. (1988). Inactivation of calcium release from the sarcoplasmic reticulum in frog skeletal muscle. *Journal of Physiology* **405**, 727–745.

TSUGORKA, A., RIOS, E. & BLATTER, L. A. (1995). Imaging elementary events of calcium release in skeletal muscle cells. *Science* **269**, 1723–1726.

Author's email address

M. F. Schneider: mschneid@umabnet.ab.umd.edu